Appl. Phys. B (2014) 115:149–153
DOI 10.1007/s00340-014-5808-z

Applied Physics B
Lasers and Optics

RAPID COMMUNICATION

Quantum-noise-limited cavity ring-down spectroscopy

D. A. Long · A. J. Fleisher · S. Wójtewicz · J. T. Hodges

Received: 23 December 2013 / Accepted: 21 February 2014 / Published online: 29 March 2014

Abstract We demonstrate a heterodyne-detected cavity ring-down spectroscopy (CRDS) method that allows for a noise-equivalent absorption coefficient of 6×10^{-14} cm^{-1} Hz$^{-1/2}$, the lowest which has been reported in a CRDS measurement. It is shown that heterodyne-detected CRDS also reaches the quantum noise limit at reasonable optical powers. In addition to offering ultra-high sensitivity, this technique provides high frequency agility over a range of 2 THz in the near-infrared, which allows entire absorption bands to be recorded in minutes. As a demonstration experiment, high resolution spectra of a near-infrared carbon dioxide band have been recorded.

Spectroscopic techniques with ultra-high sensitivity allow for the study of a wide variety of physical and chemical phenomena, ranging from the interrogation of individual atoms [1] and molecules [2, 3] to the quantitative extraction of ensemble properties from detailed molecular lineshape investigations [4, 5]. The fundamental limit to spectroscopic sensitivity is the quantum noise limit imposed by the photons themselves, often referred to as the shot-noise limit. Cavity ring-down spectroscopy (CRDS) [6] is a relatively simple technique for measuring absorption with high sensitivity, but despite its pervasiveness throughout research laboratories [7], no CRDS measurement has yet reached the sensitivity limit imposed by the quantum nature of light. In general, they have been limited by technical noise because CRDS is essentially a direct-current measurement. In light of this limitation, several research groups have explored heterodyne approaches [8, 9], including Ye and Hall [10] who developed a method in which the interference between neighboring transmission modes is recorded. Herein, we have adapted their operating principle in order to leverage recent developments in electro-optics, which allows for rapid scanning [11, 12]. The resulting instrument has reached the quantum noise limit and achieved a record sensitivity for CRDS.

Heterodyne-detected cavity ring-down spectroscopy (HD-CRDS) is performed by alternately exciting neighboring modes of an optical cavity. The resulting transmission is then measured by a high-bandwidth photoreceiver with the HD-CRDS signal being the time-varying transmitted intensity at the difference frequency of the two modes (i.e., a selected integer multiple of the cavity's free spectral range). This technique has significant advantages over traditional direct-current CRDS measurements. Firstly, HD-CRDS moves the measurement to high frequencies in order to reduce the effects of $1/f$ noise that limit traditional CRDS experiments. Secondly, traditional CRDS signals often become technical-noise-limited due to the low light levels at the tail of the decay event. Finally, HD-CRDS allows for the measurement of differential losses between two cavity modes during each build-up/decay event, thus providing a rapid and direct measure of absorption and reducing the effects of drift in the system base losses (e.g., etalon effects).

Electronic supplementary material The online version of this article (doi:10.1007/s00340-014-5808-z) contains supplementary material, which is available to authorized users.

D. A. Long (✉) · A. J. Fleisher · S. Wójtewicz · J. T. Hodges
National Institute of Standards and Technology, 100 Bureau Drive, Gaithersburg, MD 20899, USA
e-mail: david.long@nist.gov

S. Wójtewicz
Institute of Physics, Faculty of Physics, Astronomy and Informatics, Nicolaus Copernicus University, Grudziadzka 5, 87-100 Torun, Poland

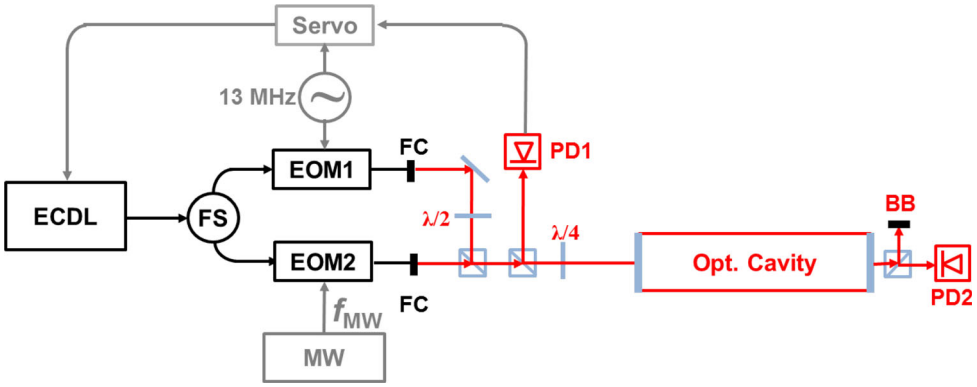

Fig. 1 Experimental setup for the described heterodyne-detected cavity ring-down spectrometer. The external-cavity diode laser (ECDL) is offset-locked to the optical cavity through the use of Pound–Drever–Hall locking [13] in a 2*f*-configuration [11] using the beam propagating through the locking electro-optic modulator (EOM1). A fast-switching microwave source (MW) drives EOM2 such that a single, selected sideband is resonant with the cavity. During a measurement, the microwave frequency (f_{MW}) is stepped in increments of the cavity's free spectral range to selectively excite individual cavity modes, thus producing the heterodyne signal. The remaining shown components are a fiber splitter (FS), fiber couplers (FC), photodiodes (PD), and a beam block (BB). Note that fiber-coupled elements are shown in *black*, free-space optics in *red*, and electronic signals in *gray*

Our present instrument has combined the operating principle of HD-CRDS with the frequency-agile rapid scanning spectroscopy (FARS) technique we have recently developed [11, 12] (see Fig. 1). Briefly, our HD-CRDS instrument utilizes a high-bandwidth, waveguide-based electro-optic phase modulator to place a series of tunable sidebands on our probe laser (an external-cavity diode laser, ECDL). The carrier frequency is continuously offset-locked using 2*f*-Pound–Drever–Hall locking [11, 13] to an optical cavity mode such that it is non-resonant but achieves a relative linewidth of 130 Hz between the probe laser and the optical cavity [11]. For traditional FARS-CRDS without heterodyne detection, we set the modulation frequency so that only a single, selected laser sideband is resonant with the cavity, thus utilizing this sideband to probe the gas sample. For HD-CRDS, we simply alternate the modulation frequency between a pair of values that are separated by a multiple of the cavity's free spectral range (203.076 MHz), leading to a heterodyne signal on the photoreceiver at the difference frequency. The temporal variation in the amplitude of the difference frequency signal yields our HD-CRDS signal (see Fig. 2). This demodulated signal can be readily modeled as the product of two out-of-phase electromagnetic fields (E_1 and E_2) [10]:

$$E_1 = 2\frac{\sqrt{P_{0,1}}}{\sqrt{2}}\left[1+\exp\left(\frac{-\Delta t}{2\tau_1}\right)-\exp\left(\frac{-t}{\tau_1}\right)\right]\text{and}$$
$$E_2 = 2\frac{\sqrt{P_{0,2}}}{\sqrt{2}}\exp\left(\frac{-t}{\tau_2}\right), \quad (1)$$

where Δt is the chopping period and $P_{0,1}$ and $P_{0,2}$ are the respective peak powers in transmission for each mode. In this expression, each field has a decay rate ($1/\tau_1$ and $1/\tau_2$) that is equal to $(L_0 + A)c/(2l)$ where c is the speed of light, l is the single-pass cavity length and L_0 and A are the single-pass intensity losses due to the mirror and absorption by the gas, respectively. For small amounts of absorption, the peak signal occurs at time $t = \tau_c \ln(2)$ with $\tau_c = \frac{2l}{cL_0}$. This gives a peak heterodyne signal of $\eta\sqrt{2}P_0/4$, where η is the detector responsivity (A/W). As derived by Ye and Hall, in the weak absorption limit and assuming the same transmitted power for each mode denoted by P_0, comparison of the peaks of two neighboring half cycles separated in time by $\Delta t/2$ gives a difference current of

$$|\Delta i| \approx \eta P_0 \frac{\ln 2}{\sqrt{2}}\frac{A}{L_0} \quad (2)$$

which is proportional to the difference in absorption between the two modes. A working expression for the measured noise-equivalent absorption coefficient (NEA) can be obtained by solving Eq. 2 for A, dividing by the cavity length l and multiplying by the square root of the averaging time t_{avg}, which we equate to $\frac{1}{2\pi B}$ where B is the detection bandwidth (Hz). We also define the observed signal-to-noise ratio as $\text{SNR} = (\eta\sqrt{2}P_0/4)/|\Delta i_{min}|$ which corresponds to the peak heterodyne signal and a one-standard-deviation noise level given by $|\Delta i_{min}|$. These assignments yield

$$\text{NEA} = \frac{L_0}{2\ln(2)\cdot\text{SNR}\cdot l\sqrt{2\pi B}}, \quad (3)$$

which can be used to compute the noise limit in terms of system observables. Here, $l = 74$ cm and $L_0 = 1.6 \times 10^{-4}$, which corresponds to a cavity finesse of

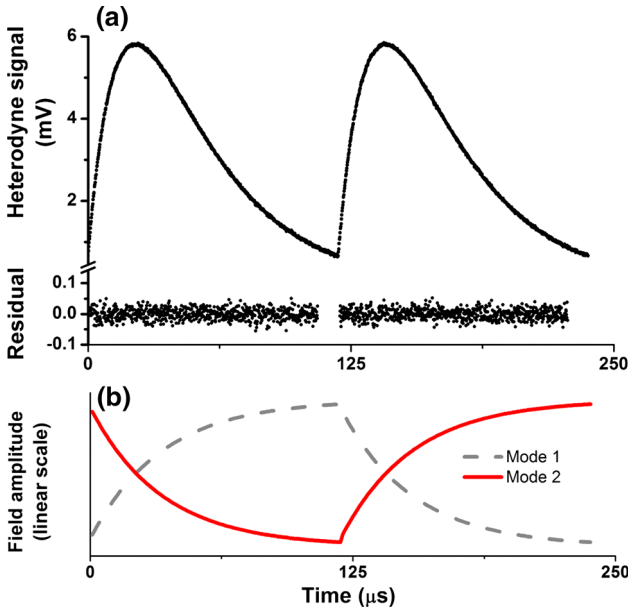

Fig. 2 Typical heterodyne signal and the corresponding (calculated) electric field amplitudes. **a** Representative empty cavity heterodyne signal for an incident power level of 29 μW recorded with the traditional InGaAs photoreceiver at a detection bandwidth of 5 MHz. This trace was recorded on a spectrum analyzer in amplitude versus time mode at a frequency of 203.076 MHz (i.e., the difference frequency). Also shown are the corresponding residuals when fitted with the model of Ye and Hall [10] with the constraint that the two modes have identical ring-down time constants. The observed signal-to-noise ratio was 340:1. **b** This panel illustrates the electric field amplitudes (Eq. 1) that correspond to the two adjacent cavity modes. The heterodyne beat between these two fields gives rise to the signal found in the *upper panel*. In the presence of absorption the two half cycles become asymmetric due to the differing time constants of the two cavity modes

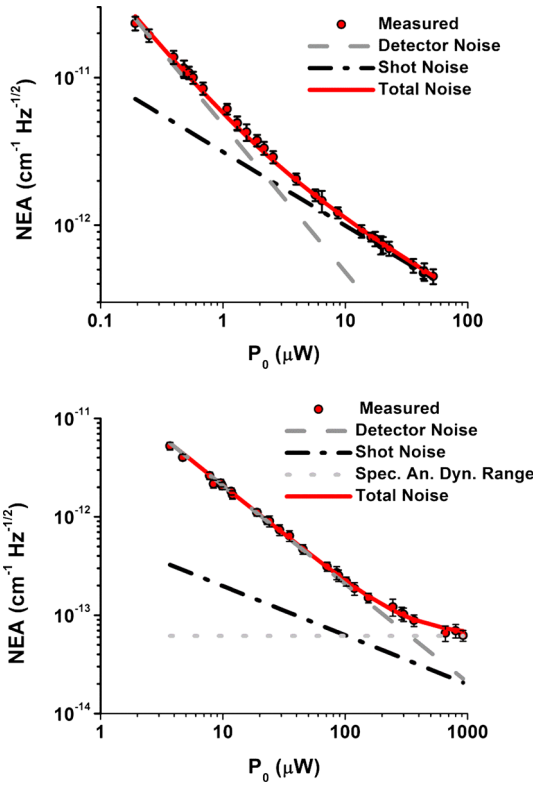

Fig. 3 Measured noise-equivalent absorption coefficient (NEA) as a function of incident optical power (P_0) for two different photoreceivers. Also shown are expanded uncertainties (2σ) and calculated noise-limited sensitivities. (*Upper panel*) Results with an avalanche photodiode having a noise-equivalent power of 3 pW Hz$^{-1/2}$ and an excess noise factor of 5. At low power levels, the observed NEA is limited by detector noise as well as by shot noise. At higher power levels (>10 μW), the measurement reaches the quantum noise limit. (*Lower panel*) Results with a traditional InGaAs photoreceiver with a noise-equivalent power of 13 pW Hz$^{-1/2}$ and no excess noise factor. Also shown is the dynamic range limit of the spectrum analyzer (Spec. An. Dyn. Range) that we used for data acquisition. These measurements reach (at the highest optical powers) within a factor of 3 of the shot-noise limit and achieve an NEA of 6×10^{-14} cm^{-1} Hz$^{-1/2}$, for a signal-to-noise ratio of 4,000:1

2×10^4. Heterodyne measurements were made with two different photoreceivers having a bandwidth of 1 GHz: an avalanche photodiode (APD) and a traditional InGaAs detector. The APD offers a lower noise-equivalent power (3 pW Hz$^{-1/2}$ vs. 13 pW Hz$^{-1/2}$) but also has a much lower saturation power and an excess noise factor, x_N, of 5. Each detector was then exposed to a wide range of incident optical power levels, P_0, in order to quantify the instrument sensitivity and interrogate the relevant noise sources (see Fig. 3). With the APD, we reached the fundamental quantum noise level (for $P_0 > 10$ μW) given by Ye and Hall as

$$\mathrm{NEA_{QN}} = \frac{x_N L_0}{\sqrt{\pi}\ln(2) l}\sqrt{\frac{e}{\eta P_0}}, \tag{4}$$

where e is the electron charge [10] and demonstrated a minimum NEA of 5×10^{-13} cm^{-1} Hz$^{-1/2}$.

Because the traditional InGaAs detector could measure higher incident powers, we were able to achieve significantly lower NEA values than with the APD. At an incident optical power of 0.9 mW, we reached an NEA of 6×10^{-14} cm^{-1} Hz$^{-1/2}$, which is a factor of 20 lower than the most sensitive CRDS experiment previously reported in the literature [14]. Unfortunately, at the highest incident power levels, we are limited by the dynamic range of the spectrum analyzer used for data acquisition. The use of a spectrum analyzer or high-speed digitizer with a wider dynamic range would provide a facile route to an even higher sensitivity.

A largely quantum-noise-limited result (within a factor of 1.5) was also reached in the initial demonstration of noise-immune, cavity-enhanced, optical-heterodyne molecular spectroscopy (NICE-OHMS) [15]. This technique, which is a dispersion measurement that is

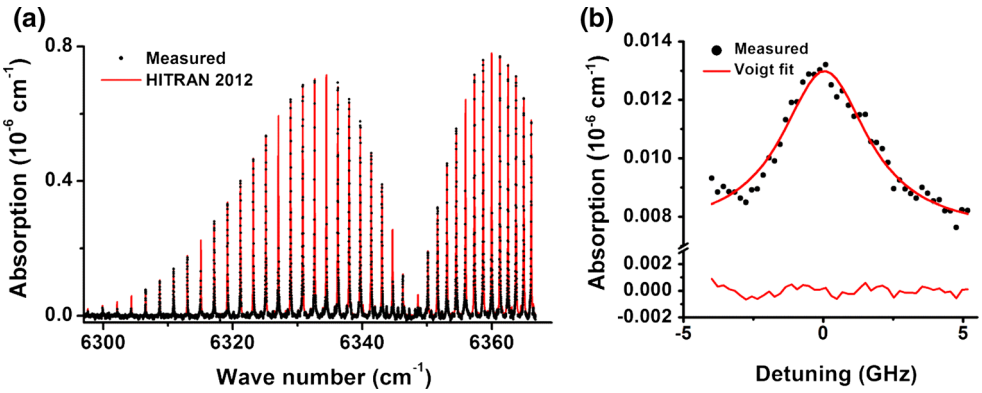

Fig. 4 Spectra of CO_2 transitions near 1,575 nm using a 425 μmol mol^{-1} CO_2 in air sample at a pressure of 51 kPa. **a** Spectrum of the (30012) ← (00001) CO_2 band with the corresponding calculated spectrum based upon the HITRAN 2012 database [21]. The baseline and an etalon have been removed. During this scan, the arbitrary waveform generator was utilized to step scan the modulation frequency across a 26-GHz-wide portion of the spectrum in 17 ms. The electro-optic modulator efficiency varied significantly across this range of frequencies (0.6–60 μW). Due to the limited efficiency of the electro-optic modulator at low frequencies, we did not utilize modulation frequencies below 2.2 GHz; this resulted in the small gaps in the measured spectrum. The laser's frequency was then coarsely adjusted (using the grating and piezoelectric transducer) approximately 60 times in order to record the shown 2 THz-wide spectrum. The small gaps could be filled by utilizing additional grating tuning steps or by adjusting the arbitrary waveform generator output amplitude as a function of frequency. **b** Measured air-broadened spectrum for the weak (30012) ← (01101) *R*5e CO_2 hot band transition having an intensity of 3.522×10^{-25} cm mol^{-1} [21]. A linear baseline has been subtracted. The shown air-broadened spectrum has a peak signal-to-noise ratio of 50:1 and was recorded in 5.5 ms (i.e., 120 μs per spectral point). The observed noise level is 4×10^{-10} cm^{-1} and corresponds to a noise-equivalent absorption coefficient, that is commensurate with those found in the lower panel of Fig. 3 for these optical power levels

sensitive to cavity mode pulling, achieved an NEA of 1×10^{-14} cm^{-1} Hz$^{-1/2}$ due to the high incident power of 5 mW (and correspondingly low shot-noise limit). NICE-OHMS and HD-CRDS share many similarities in that both rely upon heterodyne measurements of interfering transmission fields from an optical cavity. However, HD-CRDS has some significant advantages when compared to NICE-OHMS including less sensitivity to residual amplitude modulation and unbalanced sideband amplitudes. In addition, the initial demonstration of NICE-OHMS was performed with an ultra-narrow-linewidth Nd:YAG laser. Subsequent implementations with more commonly used and broader linewidth lasers (e.g., ECDLs) have achieved sensitivities, which are degraded by 2–4 orders of magnitude. The highest sensitivity which has been achieved with NICE-OHMS when using a tunable laser is only 5.6×10^{-12} cm^{-1} Hz$^{-1/2}$ [16].

Importantly, the present technique allows for rapid acquisition of spectra (unlike the original implementation by Ye and Hall [10]) due to the use of a high-bandwidth EOM instead of a pair of low-bandwidth acousto-optic modulators. With an arbitrary waveform generator (50 GS/s), we can step scan the modulation frequency applied to the electro-optic modulator and thus record a 26-GHz-wide spectrum of an individual, atmospheric-pressure-broadened transition in 17 ms (see Fig. 4). We note that the use of an arbitrary waveform generator (or other fast-switching microwave source) is required as the switching time must be significantly less than the cavity's ring-down time constant. In the absence of cavity drift, the uncertainty of the relative frequency axis of the absorption spectrum is then given simply by the relative laser linewidth (130 Hz). Entire absorption bands can also be recorded by periodically stepping the ECDL grating in order to coarsely tune the laser wavelength. In this way, a 2-THz-wide spectrum can be recorded in 20 min by dividing the spectrum into approximately 60 equal-width sections. In addition, by recording the heterodyne beat frequency between the probe laser carrier frequency and an absolute frequency reference (e.g., an optical frequency comb), an absolute frequency uncertainty at the kHz-level could be achieved [17]. Finally, we note the quantum-noise-limited NEA reported here is significantly lower than that which has been achieved using direct frequency comb spectroscopy due to the very low power per comb tooth [18] (the NEA reported by Bernhardt et al. [19] appears to be lower than that found in Ref. [18] but was incorrectly normalized to Hz$^{-1/2}$ [20]).

The described HD-CRDS instrument is well suited to investigations in optical metrology, fundamental physics, and chemical kinetics because of its unique combination of ultra-high sensitivity, high scanning rates, and broad tunability. Possible application areas include measurements of trace atmospheric species and their kinetics, tests of the symmetrization postulate, observations of highly forbidden transitions, as well as quantification of rare isotopes (e.g., clumped isotopes and radiocarbon). We believe that this

technique will allow for rapid, quantum-noise-limited absorption measurements throughout the visible and infrared spectral region and should enable transformative measurements which were not previously possible.

Acknowledgments Support was provided by an NIST Innovation in Measurement Science award and the NIST Greenhouse Gas Measurements and Climate Research Program. S. W. was partially supported by the Foundation for Polish Science TEAM Project co-financed by the EU European Regional Development Fund. We also thank H. Otten and J. Dement for loaning us the arbitrary waveform generator and offering assistance in generating the required waveforms.

References

1. A.M. Kaufman, B.J. Lester, C.A. Regal, Phys. Rev. X **2**(4), 041014 (2012)
2. W.E. Moerner, L. Kador, Phys. Rev. Lett. **62**(21), 2535–2538 (1989)
3. A. Gaiduk, M. Yorulmaz, P.V. Ruijgrok, M. Orrit, Science **330**(6002), 353–356 (2010)
4. C. Daussy, M. Guinet, A. Amy-Klein, K. Djerroud, Y. Hermier, S. Briaudeau, C.J. Bordé, C. Chardonnet, Phys. Rev. Lett. **98**(25), 250801 (2007)
5. J.M. Hartmann, H. Tran, N.H. Ngo, X. Landsheere, P. Chelin, Y. Lu, A.W. Liu, S.M. Hu, L. Gianfrani, G. Casa, A. Castrillo, M. Lepere, Q. Deliere, M. Dhyne, L. Fissiaux, Phys. Rev. A **87**(1), 013403 (2013)
6. A. O'Keefe, D.A.G. Deacon, Rev. Sci. Instrum. **59**(12), 2544–2551 (1988)
7. G. Berden, R. Peeters, G. Meijer, Int. Rev. Phys. Chem. **19**(4), 565–607 (2000)
8. M.D. Levenson, B.A. Paldus, T.G. Spence, C.C. Harb, J.S. Harris, R.N. Zare, Chem. Phys. Lett. **290**(4–6), 335–340 (1998)
9. M.D. Levenson, B.A. Paldus, T.G. Spence, C.C. Harb, R.N. Zare, M.J. Lawrence, R.L. Byer, Opt. Lett. **25**(12), 920–922 (2000)
10. J. Ye, J.L. Hall, Phys. Rev. A **61**(6), 061802 (2000)
11. D.A. Long, G.-W. Truong, R.D. Van Zee, D.F. Plusquellic, J.T. Hodges, Appl. Phys. B **114**(4), 489–495 (2014)
12. G.W. Truong, K.O. Douglass, S.E. Maxwell, R.D. van Zee, D.F. Plusquellic, J.T. Hodges, D.A. Long, Nat. Photon. **7**(7), 532–534 (2013)
13. R.W.P. Drever, J.L. Hall, F.V. Kowalski, J. Hough, G.M. Ford, A.J. Munley, H. Ward, Appl. Phys. B **31**(2), 97–105 (1983)
14. T.G. Spence, C.C. Harb, B.A. Paldus, R.N. Zare, B. Willke, R.L. Byer, Rev. Sci. Instrum. **71**(2), 347–353 (2000)
15. J. Ye, L.S. Ma, J.L. Hall, J. Opt. Soc. Am. B **15**(1), 6–15 (1998)
16. P. Ehlers, I. Silander, J. Wang, O. Axner, J. Opt. Soc. Am. B **29**(6), 1305–1315 (2012)
17. G.-W. Truong, D.A. Long, A. Cygan, D. Lisak, R.D. Van Zee, J.T. Hodges, J. Chem. Phys. **138**, 094201 (2013)
18. A. Foltynowicz, T. Ban, P. Maslowski, F. Adler, J. Ye, Phys. Rev. Lett. **107**(23), 233002 (2011)
19. B. Bernhardt, A. Ozawa, P. Jacquet, M. Jacquey, Y. Kobayashi, T. Udem, R. Holzwarth, G. Guelachvili, T.W. Hansch, N. Picque, Nat. Photon. **4**(1), 55–57 (2010)
20. N.R. Newbury, I. Coddington, W. Swann, Opt. Express **18**(8), 7929–7945 (2010)
21. L.S. Rothman, I.E. Gordon, Y. Babikov, A. Barbe, D. Chris Benner, P.F. Bernath, M. Birk, L. Bizzocchi, V. Boudon, L.R. Brown, A. Campargue, K. Chance, E.A. Cohen, L.H. Coudert, V.M. Devi, B.J. Drouin, A. Fayt, J.M. Flaud, R.R. Gamache, J.J. Harrison, J.M. Hartmann, C. Hill, J.T. Hodges, D. Jacquemart, A. Jolly, J. Lamouroux, R.J. LeRoy, G. Li, D.A. Long, O.M. Lyulin, C.J. Mackie, S.T. Massie, S. Mikhailenko, H.S.P. Müller, O.V. Naumenko, A.V. Nikitin, J. Orphal, V. Perevalov, A. Perrin, E.R. Polovtseva, C. Richard, M.A.H. Smith, E. Starikova, K. Sung, S. Tashkun, J. Tennyson, G.C. Toon, V.G. Tyuterev, G. Wagner, J. Quant. Spectrosc. Radiat. Transfer **130**, 4–50 (2013)